Author Manuscript

Author Manuscript

Author Manuscript

Author Manuscript

HHS Public Access

Author manuscript

J Am Chem Soc. Author manuscript; available in PMC 2024 March 01.

Published in final edited form as:

J Am Chem Soc. 2023 March 01; 145(8): 4784–4790. doi:10.1021/jacs.2c13615.

Direct Proton-Coupled Electron Transfer between Interfacial Tyrosines in Ribonucleotide Reductase

Jiayun Zhong[†], **Clorice R. Reinhardt**[‡], **Sharon Hammes-Schiffer**[†]

[†]Department of Chemistry, Yale University, New Haven, Connecticut 06520, United States

[‡]Department of Molecular Biophysics and Biochemistry, Yale University, New Haven, Connecticut 06520, United States

Abstract

Ribonucleotide reductase (RNR) regulates DNA synthesis and repair in all organisms. The mechanism of *Escherichia coli* RNR requires radical transfer over a proton-coupled electron transfer (PCET) pathway spanning ~32 Å across two protein subunits. A key step along this pathway is the interfacial PCET reaction between Y356 in the β subunit and Y731 in the α subunit. Herein this PCET reaction between two tyrosines across an aqueous interface is explored with classical molecular dynamics and quantum mechanical/molecular mechanical (QM/MM) free energy simulations. The simulations suggest that the water-mediated mechanism involving double proton transfer through an intervening water molecule is thermodynamically and kinetically unfavorable. The direct PCET mechanism between Y356 and Y731 becomes feasible when Y731 is flipped toward the interface and is predicted to be approximately isoergic with a relatively low free energy barrier. This direct mechanism is facilitated by hydrogen bonding of water to both Y356 and Y731. These simulations provide fundamental insights into radical transfer across aqueous interfaces.

GRAPHICAL ABSTRACT

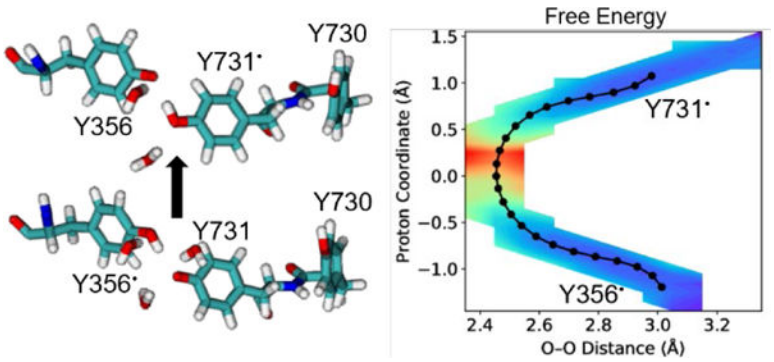

Corresponding Author: Sharon Hammes-Schiffer, sharon.hammes-schiffer@yale.edu.

ASSOCIATED CONTENT

Supporting Information: Simulation details and additional analyses of classical molecular dynamics and QM/MM string simulations.

Author Manuscript Author Manuscript Author Manuscript Author Manuscript

INTRODUCTION

Ribonucleotide reductase (RNR) is critical for DNA synthesis and repair in all living organisms,[1–4] making it a target for cancer therapies.[5–6] RNR catalyzes the reduction of ribonucleotides to deoxyribonucleotides through an initiating thiyl radical (Figure 1). In *E. coli* RNR, a proton-coupled electron transfer (PCET) pathway consisting of Y122β ↔ [W48β] ↔ Y356β ↔ Y731α ↔ Y730α ↔ C439α generates a series of tyrosyl radicals that eventually produces this critical thiyl radical.[2, 4] This PCET pathway spans ~32 Å across both the α and β subunits of RNR. A key step along this pathway is the interfacial PCET reaction between Y356β and Y731α, which is not yet well understood. Recently a 3.6 Å resolution cryo-EM structure of the α2β2 complex of *E. coli* RNR was solved.[7] This structure is asymmetric in that the α/β pair is in the pre-turnover state with an intact PCET pathway, whereas the α′/β′ pair is in the post-turnover state (Figure 1). Within this structure, Y731 is observed to be stacked with the adjacent Y730 in the α subunit, and the distance between the oxygen atoms of Y731 in the α subunit and Y356 in the β subunit is 8.3 Å.[7] Our previous molecular dynamics (MD) simulations[8] based on this cryo-EM structure suggest that Y731 can flip out and point toward the α/β subunit interface, as also observed in spectroscopic experiments [9–10] and in a crystal structure of a modified α subunit[11] and in another species.[12] These spectroscopic experiments[10] and our free energy simulations[8] have indicated that both conformations can be sampled at room temperature.

Prior experimental studies[13–16] and MD simulations[8] have implicated water molecules hydrogen bonded to Y356 and Y731. Moreover, our previous quantum mechanical/molecular mechanical (QM/MM) free energy simulations suggested that a glutamate residue mediates PCET between Y731 and Y730 through a proton relay mechanism.[17] The significant distance between the oxygen atoms of Y356 and Y731 in the cryo-EM structure,[7] in conjunction with the experimental and theoretical evidence of water molecules hydrogen bonding to both Y356 and Y731,[8, 13–14] suggests that water could play a similar role in the interfacial PCET reaction between Y356 and Y731 and serve as a mediator in a proton relay between these tyrosines. However, a recent electron-nuclear double resonance (ENDOR) experiment using fluorinated Y731 measured the distance between the oxygen atoms of Y356 and Y731 to be ~3 Å when Y731 is flipped out toward the α/β interface, supporting the possibility of a direct PCET mechanism.[15] A previous computational study on a model system of two stacked tyrosines showed that direct PCET has a lower free energy barrier than a water-mediated mechanism.[18] Furthermore, as shown by our previous QM/MM free energy simulations of the PCET reaction between Y730 and C439, water can influence the free energy barrier and reaction free energy through hydrogen-bonding interactions without directly participating in a proton relay process as a mediator.[19]

Herein, we investigate the interfacial PCET reaction between Y356 and Y731 in RNR using a combination of classical MD and QM/MM free energy simulations. In contrast to our previous classical MD simulations, where the radical was on Y122,[8] we perform MD simulations with the radical on either Y356 or Y731 and analyze the distance between these two residues and their hydrogen-bonding interactions with surrounding water molecules. Subsequently, we conduct QM/MM free energy simulations of PCET between Y356 and Y731 to determine whether this PCET reaction occurs with Y731 in its stacked or flipped

Author Manuscript Author Manuscript Author Manuscript Author Manuscript

conformation and whether an intervening water molecule serves as a mediator in a proton relay mechanism (Scheme 1). The simulations provide evidence for direct interfacial PCET between Y356 and Y731 in its flipped conformation.

METHODS

All simulations started from the cryo-EM structure of the active α2β2 complex of *E.coli* RNR (PDB ID: 6W4X).[7] Note that the local resolution of this structure varies from 3.3 to 5.5 Å, but the region of the intact PCET pathway across the α/β interface is ~3.3 Å resolution. The protein was immersed in a box of explicit TIP3P water[20] molecules and neutralized with Na^+ followed by addition of 150 mM NaCl. The system preparation and equilibration protocols were adapted from our previous MD simulations of RNR,[8] and the details are described in the Supporting Information (SI). We propagated classical MD trajectories for the solvated RNR complex with the radical on either Y356, denoted Y356$^\bullet$ simulations, or on Y731, denoted Y731$^\bullet$ simulations. To ensure adequate sampling, we generated eight independent 100 ns trajectories for the Y356$^\bullet$ and Y731$^\bullet$ simulations, each with different initial conditions.

We conducted QM/MM finite temperature string simulations with umbrella sampling[21–22] to calculate the free energy surfaces for both water-mediated and direct PCET between Y356 and Y731. The initial conformations with Y731 in the flipped conformation were obtained from the classical MD simulations described above and in the SI, and the initial conformations with Y731 in the stacked conformation were obtained from our previous MD simulations with a restraint on the Y731$^\bullet$ sidechain.[23] The QM region was described with the ωB97X-D functional[24] and the 6–31+G** basis set,[25–27] and the MM region was described with the AMBER ff14SB force field.[28–31] This level of theory was shown to be consistent with multireference complete active space self-consistent field calculations with second-order perturbative corrections (CASSCF+NEVPT2) for PCET between two tyrosine molecules in our previous work.[17] We used the AMBER/Q-CHEM interface[32–34] to perform the QM/MM free energy simulations. Additional details about the QM/MM free energy simulations are provided in the SI.

RESULTS AND DISCUSSION

We analyzed the Y731 conformation and the distance between Y356 and Y731 for the combined classical MD data. Y731 was observed to be in the flipped conformation for more than 70% of the conformations sampled, and the stacked conformation of Y731 was not observed (Figure S3). This finding is consistent with previous MD simulations with the radical on Y122, denoted Y122$^\bullet$ simulations, where a restraint on the Y731 sidechain dihedral angle was necessary to adequately sample the stacked conformation.[8] Y356 and Y731 were found to be ~2–3 Å closer to each other for the Y356$^\bullet$ and Y731$^\bullet$ simulations, compared to the previous Y122$^\bullet$ simulations. Specifically, the average distance between the Y356 and Y731 oxygen atoms is 5.1 ± 2.1 Å and 5.9 ± 2.6 Å for the Y356$^\bullet$ and Y731$^\bullet$ simulations, respectively, compared to 8.0 ± 1.6 Å for the Y122$^\bullet$ simulations (Figure S3). We observed that this distance is < 3.5 Å for 15 % and 23 % of the conformations sampled when the radical is on Y356 and Y731, respectively. A recent ENDOR spectroscopic study

Author Manuscript Author Manuscript Author Manuscript Author Manuscript

using a F2Y731 variant of RNR measured this distance to be ~3 Å when Y731 is flipped toward the α/β interface.[15]

We also used the classical MD simulations to investigate hydrogen-bonding interactions between Y356 and Y731 and surrounding water molecules. Y731, Y731•, Y356, and Y356• hydrogen bond to at least one water molecule for 68%, 44%, 54%, and 30%, respectively, of the conformations sampled (Figure 2). As discussed below, these hydrogen-bonded water molecules can significantly influence the thermodynamics and kinetics of the PCET reaction. Moreover, these hydrogen-bonding interactions are consistent with previous ENDOR spectroscopic studies.[13–15] Y356 and Y356• were found to hydrogen bond to R411 for 1% and 12%, respectively, of the conformations sampled. As mentioned above, ~15 to 23% of the conformations sampled exhibited an oxygen-oxygen distance between the two tyrosines less than 3.5 Å, potentially favoring the direct PCET mechanism. In comparison, only 0.16% and 2.27% of the conformations sampled for the Y356• and Y731• simulations, respectively, exhibited a bridging water between Y356 and Y731 with the hydrogen atoms oriented in a manner favorable to a proton relay water-mediated mechanism (Scheme 1).

Following the classical MD simulations, we performed QM/MM free energy simulations to compute the free energy surfaces for both water-mediated and direct PCET. We simulated four independent strings corresponding to different mechanisms and conformations. The water-mediated PCET mechanism, where a bridging water molecule was located between Y356 and Y731, was investigated for both the stacked and flipped Y731 conformations. The direct PCET mechanism, where the distance between the oxygen atoms of Y356 and Y731 was ~3.0 Å, was only investigated for the flipped Y731 because the proton donor-acceptor distance was not short enough to allow for direct PCET when Y731 was in the stacked conformation. Previously we computed the free energy profiles for the conformational change between the flipped and stacked conformation of Y731 in its standard[8] and radical forms (see Figure S20 of Ref. [23]). These previous simulations showed that both the stacked and flipped conformations are thermally accessible at room temperature with a relatively low free energy barrier for interconversion. Moreover, this interconversion is relatively local in that it does not require other significant conformational changes from the cryo-EM structure.[7–8] Two different initial conformations of the surrounding water were explored for the direct PCET mechanism. The QM region included the sidechains of Y356 and Y731 for all strings, as well as the bridging water for the water-mediated mechanisms and the sidechain of Y730 for the stacked Y731 conformation (Figure S1). Representative reactant and product conformations for the four strings simulated are shown in Figure 3.

The free energy barriers and reaction free energies for the mechanisms studied are given in Table 1. Both water-mediated PCET mechanisms are significantly endoergic with high free energy barriers, suggesting that these mechanisms are not likely. The barrier is higher for the stacked Y731 conformation but would be inaccessible for the flipped Y731 conformation as well. We also found that the two protons transfer concertedly in the double proton transfer process for both conformations of Y731 in the water-mediated PCET mechanism (Figure S7). The two direct PCET mechanisms have much lower free energy barriers and reaction free energies. The most favorable mechanism is isoergic with a free energy barrier of 9.0 kcal/mol. Previous pulsed electron–electron double resonance and EPR spectroscopy

Author Manuscript Author Manuscript Author Manuscript Author Manuscript

experiments led to an estimated reaction free energy of 2.6 ± 1.2 kcal/mol for radical transfer from Y356 to Y731.[35] Our most thermodynamically and kinetically favorable QM/MM string simulation predicts a reaction free energy ranging from ca. 0 to 1.0 kcal/mol over the last 30 iterations (Figures S4 and S6). Given the uncertainties in both the experimental and computational estimates, the simulation results are considered to be qualitatively consistent with the experimental results.

To examine the role of water molecules in the direct PCET mechanism, we propagated two independent direct-flipped mechanism strings with different water distributions around the tyrosines (Figures 3A, 3B). The direct-flipped-1 string has a significantly lower free energy barrier and lower reaction free energy, in that it is isoergic, than the direct-flipped-2 string, which is endoergic (Table 1). These differences can be explained in terms of the relative number of hydrogen-bonding interactions between Y731 and water molecules at the top of the barrier and the product compared to the reactant (Table 2). For the direct-flipped-1 string, the additional hydrogen-bonding interaction between Y731 and water at the top of the barrier compared to the reactant state lowers the free energy barrier (Figure 4). Similarly, the additional hydrogen-bonding interaction between Y731 and water in the product compared to the reactant lowers the reaction free energy. In contrast, the direct-flipped-2 string exhibits the same number of hydrogen-bonding interactions between water and Y731 in the reactant and at the top of the barrier and exhibits one less hydrogen-bonding interaction in the product, leading to a higher free energy barrier and reaction free energy than those observed for the direct-flipped-1 string. The increase in free energy barrier and reaction free energy of ~7 and 8 kcal/mol, respectively, for the direct-flipped-2 string compared to the direct-flipped-1 string is consistent with the energies of these types of hydrogen-bonding interactions.

According to our classical MD simulations discussed above, one or two water molecules can hydrogen bond to both Y356 and Y731 with reasonable probability. As shown in Figure 2, however, hydrogen bonding to two water molecules is less likely when the tyrosine is in its radical form and is less likely for Y356 than for Y731. In contrast to Y731, Y356 remains hydrogen bonded to one water molecule throughout the direct-flipped-1 string and to no water molecules throughout the direct-flipped-2 string, thus not influencing the relative number of hydrogen bonds along the PCET reaction pathway. In both direct-flipped strings, water molecules hydrogen-bonding to Y731/Y731$^{\bullet}$ are more likely to reorient or even move away from this tyrosine compared to the water hydrogen bonding to Y356/Y356$^{\bullet}$ in the direct-flipped-1 string. Based on our analysis of these two representative strings, we observed that water molecules hydrogen bonding to Y731/Y731$^{\bullet}$ are also hydrogen bonding to more surrounding water molecules and residues, including R411, compared to the water hydrogen bonding to Y356/Y356$^{\bullet}$. The competing hydrogen-bonding interactions may lead to more dynamic hydrogen bonds between water molecules and Y731/Y731$^{\bullet}$. Additionally, in the direct-flipped-2 string, one of the water molecules hydrogen bonded to Y731 moves further away when the radical transfers to Y731, allowing the other hydrogen-bonding water molecule to reposition itself to facilitate its hydrogen-bonding interaction with Y731$^{\bullet}$.

These QM/MM free energy simulations focused on PCET between Y356 and Y731 starting from MD simulations based on the cryo-EM structure.[7] This computational methodology

Author Manuscript Author Manuscript Author Manuscript Author Manuscript

will not capture global conformational changes that occur on a relatively long timescale because of limitations in conformational sampling due to the computational expense. The QM/MM free energy simulations generate the free energy surface for the reversible PCET process between Y356 and Y731 without a preference for either direction, except that they were performed in the context of the initial cryo-EM structure, where the α/β pair with the intact PCET pathway is in the pre-turnover state. Given the short timescale of the simulations, they cannot describe slower conformational changes that occur between forward and reverse radical transfer. In this context, we did not observe any significant structural changes at the α/β interface along the simulated PCET reaction pathways. Similarly, the calculated free energy surfaces are influenced by the initial water conformations due to sampling limitations, leading to differences between the two direct-flipped mechanism strings. The PCET reaction is expected to be dominated by the more thermodynamically and kinetically favorable conformations, corresponding to the direct-flipped-1 mechanism. However, other mechanistic possibilities, such as participation of buffer molecules present in biochemical assays,[36] were not considered in this work. These simulations also do not elucidate the proton transport process from the α/β interface to bulk solvent. Furthermore, these simulations do not provide information about the other PCET reactions along the pathway or insights into the global thermodynamics of radical propagation in RNR. Such insights will most likely rely on kinetic modeling, as performed in our previous work for photosensitized RNRs within the α subunit using a combination of computational and experimental input.[23]

CONCLUSION

In summary, we computed free energy surfaces for the key interfacial PCET reaction between Y356 and Y731 in RNR using QM/MM string simulations. Our results indicate that a direct PCET mechanism with Y731 flipped out toward the α/β interface is thermodynamically and kinetically favorable compared to a water-mediated mechanism involving concerted double proton transfer. Radical transfer from Y356 to Y731 is predicted to be isoergic or slightly endoergic, qualitatively consistent with spectroscopic estimates,[35] with a free energy barrier of ~9 kcal/mol. This radical transfer is facilitated by persistent hydrogen bonding of Y356 and Y731 with water molecules. The presence of interacting water near these residues is consistent with spectroscopic experiments.[13–15] Hydrogen tunneling and nonadiabaticity are also expected to play a role in this PCET reaction.[37] Understanding this interfacial PCET step between the two subunits of RNR is essential for controlling and modifying the radical transfer pathway in this biochemically important enzyme.

Supplementary Material

Refer to Web version on PubMed Central for supplementary material.

ACKNOWLEDGMENT

This work was supported by the National Institutes of Health Grant No. R35 GM139449. This work utilized Expanse at the San Diego Supercomputer Center through allocation TG-MCB120097 from the Extreme Science and Engineering Discovery Environment (XSEDE),[38] which was supported by National Science Foundation grant

Author Manuscript Author Manuscript Author Manuscript Author Manuscript

#1548562. This work used resources on Expanse at the San Diego Supercomputer Center through allocation TG-MCB120097 from the Advanced Cyberinfrastructure Coordination Ecosystem: Services & Support (ACCESS) program, which is supported by National Science Foundation grants #2138259, #2138286, #2138307, #2137603, and #2138296. C. R. R was supported by the National Science Foundation Graduate Research Fellowship Program under Grant No. DGE1752134. We thank Alexander Soudackov, Daniel Konstantinovsky, Qiwen Zhu, and Benjamin Rousseau for technical assistance and helpful discussions. We are also grateful to JoAnne Stubbe for her valuable insights.

REFERENCES

(1). Stubbe J; Nocera DG; Yee CS; Chang MCY, Radical initiation in the class I ribonucleotide reductase: Long-range proton-coupled electron transfer? Chem. Rev 2003, 103, 2167–2202. [PubMed: 12797828]

(2). Minnihan EC; Nocera DG; Stubbe J, Reversible, Long-Range Radical Transfer in E. coli Class Ia Ribonucleotide Reductase. Acc. Chem. Res 2013, 46, 2524–2535. [PubMed: 23730940]

(3). Högbom M; Sjöberg BM; Berggren G, Radical Enzymes. eLS 2020, 1, 375–393.

(4). Greene BL; Kang G; Cui C; Bennati M; Nocera DG; Drennan CL; Stubbe J, Ribonucleotide Reductases: Structure, Chemistry, and Metabolism Suggest New Therapeutic Targets. Annu. Rev. Biochem 2020, 89, 45–75. [PubMed: 32569524]

(5). Aye Y; Li M; Long M; Weiss R, Ribonucleotide reductase and cancer: biological mechanisms and targeted therapies. Oncogene 2015, 34, 2011–2021. [PubMed: 24909171]

(6). Misko TA; Liu YT; Harris ME; Oleinick NL; Pink J; Lee HY; Dealwis CG, Structure-guided design of anti-cancer ribonucleotide reductase inhibitors. J. Enzyme Inhib. Med. Chem 2019, 34, 438–450. [PubMed: 30734609]

(7). Kang G; Taguchi AT; Stubbe J; Drennan CL, Structure of a trapped radical transfer pathway within a ribonucleotide reductase holocomplex. Science 2020, 368, 424–427. [PubMed: 32217749]

(8). Reinhardt CR; Li P; Kang G; Stubbe J; Drennan CL; Hammes-Schiffer S, Conformational Motions and Water Networks at the α/β Interface in E. coli Ribonucleotide Reductase. J. Am. Chem. Soc 2020, 142, 13768–13778. [PubMed: 32631052]

(9). Kasanmascheff M; Lee W; Nick TU; Stubbe J; Bennati M, Radical transfer in E coli ribonucleotide reductase: a NH2Y731/R411A-α mutant unmasks a new conformation of the pathway residue 731. Chem. Sci 2016, 7, 2170–2178. [PubMed: 29899944]

(10). Greene BL; Taguchi AT; Stubbe J; Nocera DG, Conformationally Dynamic Radical Transfer within Ribonucleotide Reductase. J. Am. Chem. Soc 2017, 139, 16657–16665. [PubMed: 29037038]

(11). Minnihan EC; Seyedsayamdost MR; Uhlin U; Stubbe JJ, Kinetics of Radical Intermediate Formation and Deoxynucleotide Production in 3-Aminotyrosine-Substituted Escherichia coli Ribonucleotide Reductases. J. Am. Chem. Soc 2011, 133, 9430. [PubMed: 21612216]

(12). Rehling D; Scaletti ER; Grinberg IR; Lundin D; Sahlin M; Hofer A; Sjöberg B-M; Stenmark P, Structural and Biochemical Investigation of Class I Ribonucleotide Reductase from the Hyperthermophile Aquifex aeolicus. Biochemistry 2022, 61, 92–106. [PubMed: 34941255]

(13). Nick TU; Ravichandran KR; Stubbe J; Kasanmascheff M; Bennati M, Spectroscopic Evidence for a H Bond Network at Y356 Located at the Subunit Interface of Active E. Coli Ribonucleotide Reductase. Biochemistry 2017, 56, 3647–3656. [PubMed: 28640584]

(14). Hecker FS, J.; Bennati M, Detection of Water Molecules on the Radical Transfer Pathway of Ribonucleotide Reductase by 17O Electron–Nuclear Double Resonance Spectroscopy. J. Am. Chem. Soc 2021, 143, 7237–7241. [PubMed: 33957040]

(15). Meyer A; Kehl A; Cui C; Reichardt F; Hecker F; Funk LM; Ghosh MK; Pan KT; Urlaub H; Tittmann K; Stubbe J; Bennati M, 19F Electron-Nuclear Double Resonance Reveals Interaction between Redox-Active Tyrosines across the α/β Interface of E. coli Ribonucleotide Reductase. J. Am. Chem. Soc 2022, 144, 11270–11282. [PubMed: 35652913]

(16). Nick TU; Lee W; Koßmann S; Neese F; Stubbe J; Bennati M, Hydrogen Bond Network between Amino Acid Radical Intermediates on the Proton-Coupled Electron Transfer Pathway of E. coli α2 Ribonucleotide Reductase. J. Am. Chem. Soc 2015, 137, 289–298. [PubMed: 25516424]

Author Manuscript Author Manuscript Author Manuscript Author Manuscript

(17). Reinhardt CR; Sayfutyarova ER; Zhong J; S., H.-S., Glutamate Mediates Proton-Coupled Electron Transfer Between Tyrosines 730 and 731 in Escherichia coli Ribonucleotide Reductase. J. Am. Chem. Soc 2021, 143, 6054–6059. [PubMed: 33856807]

(18). Kaila VRI; Hummer G, Energetics of Direct and Water-Mediated Proton-Coupled Electron Transfer. J. Am. Chem. Soc 2011, 133, 19040–19043. [PubMed: 21988482]

(19). Zhong J; Reinhardt CR; Hammes-Schiffer S, Role of Water in Proton-Coupled Electron Transfer between Tyrosine and Cysteine in Ribonucleotide Reductase. J. Am. Chem. Soc 2022, 144, 7208–7214. [PubMed: 35426309]

(20). Jorgensen WLC, J.; Madura JD; Impey RW; Klein ML, Comparison of simple potential functions for simulating liquid water. J. Chem. Phys 1983, 79, 926–935.

(21). Rosta E; Nowotny M; Yang W; Hummer G, Catalytic mechanism of RNA backbone cleavage by ribonuclease H from quantum mechanics/molecular mechanics simulations. J. Am. Chem. Soc 2011, 133, 8934–41. [PubMed: 21539371]

(22). Ganguly A; Thaplyal P; Rosta E; Bevilacqua PC; Hammes-Schiffer S, Quantum mechanical/molecular mechanical free energy simulations of the self-cleavage reaction in the hepatitis delta virus ribozyme. J. Am. Chem. Soc 2014, 136, 1483–1496. [PubMed: 24383543]

(23). Reinhardt CR; Konstantinovsky D; Soudackov AV; Hammes-Schiffer S, Kinetic model for reversible radical transfer in ribonucleotide reductase. Proc. Natl. Acad. Sci 2022, 119, e2202022119. [PubMed: 35714287]

(24). Chai J-D; Head-Gordon M, Long-range corrected hybrid density functionals with damped atom–atom dispersion corrections. Phys. Chem. Chem. Phys 2008, 10, 6615–6620. [PubMed: 18989472]

(25). Hehre WJ; Ditchfield R; Pople JA, Self-consistent molecular orbital methods. XII. Further extensions of Gaussian—type basis sets for use in molecular orbital studies of organic molecules. J. Chem. Phys 1972, 56, 2257–2261.

(26). Harihara Pc; Pople JA, Influence of Polarization Functions on Molecular-Orbital Hydrogenation Energies. Theor. Chim. Acta 1973, 28, 213–222.

(27). Clark T; Chandrasekhar J; Spitznagel GW; Schleyer PVR, Efficient diffuse function-augmented basis sets for anion calculations. III. The 3–21+G basis set for first-row elements, Li–F. J. Comput. Chem 1983, 4, 294–301.

(28). Cornell WD; Cieplak P; Bayly CI; Gould IR; Merz KM; Ferguson DM; Spellmeyer DC; Fox T; Caldwell JW; Kollman PA, A Second Generation Force Field for the Simulation of Proteins, Nucleic Acids, and Organic Molecules. J. Am. Chem. Soc 1995, 117, 5179–5197.

(29). Cheatham TE; Cieplak P; Kollman PA, A Modified Version of the Cornell et al. Force Field with Improved Sugar Pucker Phases and Helical Repeat. J. Biomol. Struct. Dyn 1999, 16, 845–862. [PubMed: 10217454]

(30). Hornak V; Abel R; Okur A; Strockbine B; Roitberg A; Simmerling C, Comparison of multiple Amber force fields and development of improved protein backbone parameters. Proteins 2006, 65, 712–725. [PubMed: 16981200]

(31). Maier JA; Martinez C; Kasavajhala K; Wickstrom L; Hauser KE; Simmerling C, ff14SB: Improving the Accuracy of Protein Side Chain and Backbone Parameters from ff99SB. J. Chem. Theory Comput 2015, 11, 3696–3713. [PubMed: 26574453]

(32). Case DA; Cheatham TE; Darden T; Gohlke H; Luo R; Merz KM; Onufriev A; Simmerling C; Wang B; Woods RJ, The Amber biomolecular simulation programs. J. Comput. Chem 2005, 26, 1668–1688. [PubMed: 16200636]

(33). Gotz AW; Clark MA; Walker RC, An extensible interface for QM/MM molecular dynamics simulations with AMBER. J. Comput. Chem 2014, 35, 95–108. [PubMed: 24122798]

(34). Shao Y; Gan Z; Epifanovsky E; Gilbert AT; Wormit M; Kussmann J; Lange AW; Behn A; Deng J; Feng X; Ghosh D; Goldey MB; Horn PR; Jacobson L; Kaliman I; Khaliullin RZ; Kus T; Landau A; Liu J; Proynov EI; Rhee YM; Richard RM; Rohrdanz MA; Steele RP; Sundstrom E; Woodcock HL; Zimmerman PM; Zuev D; Albrecht BJ; Alguire EC; Austin B; Beran GJ; Bernard YA; Berquist EJ; Brandhorst K; Bravaya KB; Brown ST; Casanova D; Chang C; Chen Y; Chien S; Closser KD; Crittenden DL; Diedenhofen M; Distasio RA; Do H; Dutoi AD; Edgar RG; Fatehi S; Fusti-Molnar L; Ghysels A; Golubeva-Zadorozhnaya A; Gomes J; Hanson-Heine

Author Manuscript Author Manuscript Author Manuscript Author Manuscript

MW; Harbach PH; Hauser AW; Hohenstein EG; Holden ZC; Jagau T; Ji H; Kaduk BJ; Khistyaev K; Kim J; Kim J; King RA; Klunzinger PE; Kosenkov D; Kowalczyk T; Krauter CM; Lao KU; Laurent AD; Lawler KV; Levchenko SV; Lin CY; Liu F; Livshits E; Lochan RC; Luenser A; Manohar P; Manzer SF; Mao S; Mardirossian N; Marenich AV; Maurer SA; Mayhall NJ; Neuscamman E; Oana CM; Olivares-Amaya R; O'Neill DP; Parkhill JA; Perrine TM; Peverati R; Prociuk A; Rehn DR; Rosta E; Russ NJ; Sharada SM; Sharma S; Small DW; Sodt AJ; Stein T; Stück D; Su Y; Thom AJ; Tsuchimochi T; Vanovschi V; Vogt L; Vydrov OA; Wang T; Watson M; Wenzel J; White AF; Williams CF; Yang J; Yeganeh S; Yost S; You Z; Zhang IY; Zhang X; Zhao Y; Brooks BR; Chan GK; Chipman DM; Cramer CJ; Goddard WA; Gordon MS; Hehre WJ; Klamt A; Schaefer HF; Schmidt MW; Sherrill CD; Truhlar DG; Warshel A; Xu X; Aspuru-Guzik A; Baer R; Bell AT; Besley NA; Chai J; Dreuw A; Dunietz BD; Furlani TR; Gwaltney SR; Hsu C; Jung Y; Kong J; Lambrecht DS; Liang W; Ochsenfeld C; Rassolov VA; Slipchenko LV; Subotnik JE; Van Voorhis T; Herbert JM; Krylov AI; Gill PM; Head-Gordon M, Advances in molecular quantum chemistry contained in the Q-Chem 4 program package. Molecular Physics 2015, 113, 184–215.

(35). Yokoyama K; Smith AA; Corzilius B; Griffin RG; Stubbe J, Equilibration of Tyrosyl Radicals (Y356•, Y731•, Y730•) in the Radical Propagation Pathway of the Escherichia coli Class Ia Ribonucleotide Reductase. J. Am. Chem. Soc 2011, 133, 18420–18432. [PubMed: 21967342]

(36). Shi Q; Pei Z; Song J; Li S-J; Wei D; Coote ML; Lan Y, Diradical Generation via Relayed Proton-Coupled Electron Transfer. J. Am. Chem. Soc 2022, 144, 3137–3145. [PubMed: 35133141]

(37). Harshan AK; Yu T; Soudackov AV; Hammes-Schiffer S, Dependence of Vibronic Coupling on Molecular Geometry and Environment: Bridging Hydrogen Atom Transfer and Electron–Proton Transfer. J. Am. Chem. Soc 2015, 137, 13545–13555. [PubMed: 26412613]

(38). Towns J; Cockerill T; Dahan M; Foster I; Gaither K; Grimshaw A; Hazlewood V; Lathrop S; Lifka D; Peterson GD, XSEDE: accelerating scientific discovery. Comput. Sci. Eng 2014, 16, 62–74.

Author Manuscript Author Manuscript Author Manuscript Author Manuscript

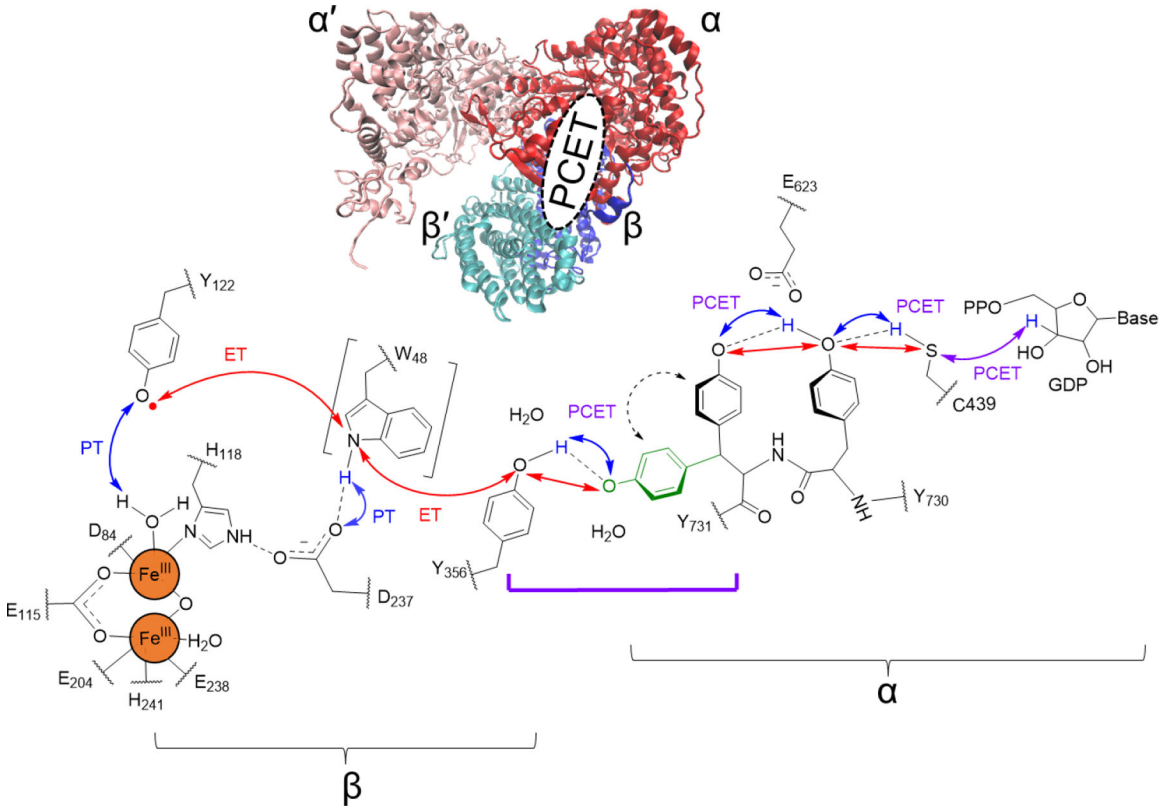

Figure 1.

Cryo-EM structure of the α2β2 complex (top) and ordered PCET pathway in the active form of *E. coli* RNR. The role of W48 and its possible proton transfer partner is unresolved and therefore is shown in black square brackets. Double-headed arrows indicate ET (electron transfer, red) and PT (proton transfer, blue), and the collinear PCET steps are labeled in purple. Both the stacked (black) and flipped-out (green) conformations of Y731 are depicted. The interfacial PCET reaction between Y356 and Y731 is indicated with a purple square bracket. Water molecules were found to hydrogen bond to both of these tyrosines in spectroscopic experiments and classical MD simulations. Proton transfer to water molecules at the α/β interface and proton transport to bulk solvent are not shown here.

Author Manuscript Author Manuscript Author Manuscript Author Manuscript

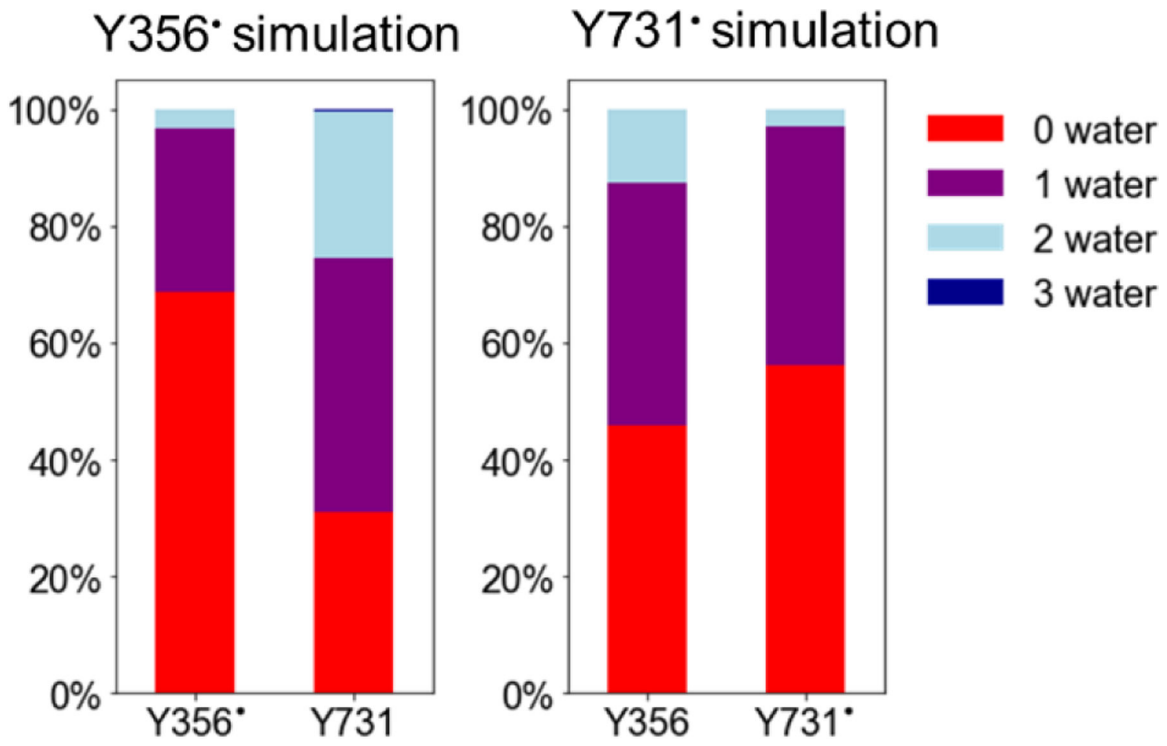

Figure 2.
Percentage of conformations with 0, 1, 2, and 3 water molecules hydrogen bonding to Y356 and Y731 when the radical is on either Y356 (left) or Y731 (right).

Author Manuscript Author Manuscript Author Manuscript Author Manuscript

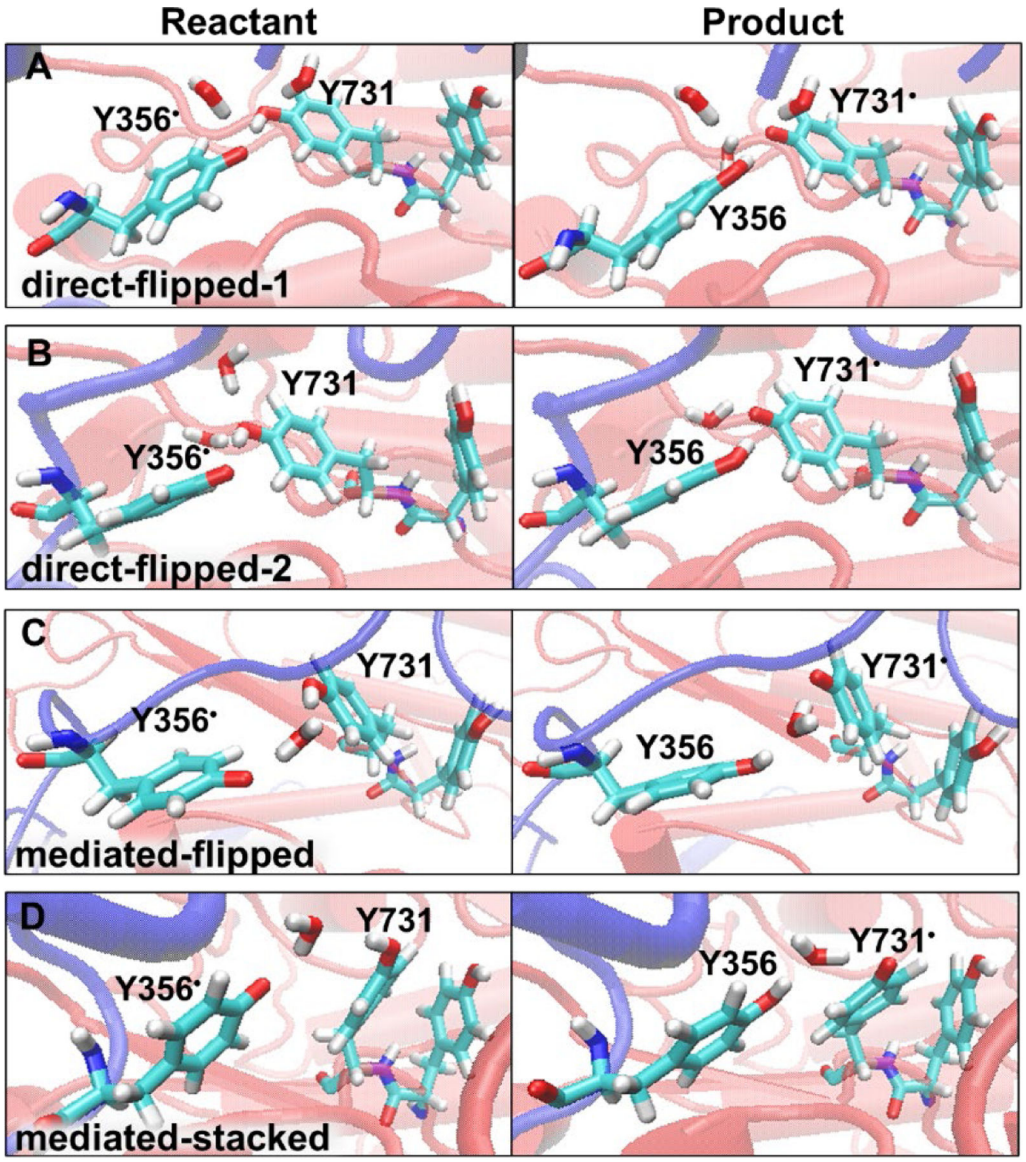

Figure 3.

Reactant and product conformations obtained from each of the four strings simulating radical transfer from Y356 to Y731. (A) direct-flipped-1 string, with one water hydrogen bonded to Y356 for both reactant and product and one water and two waters hydrogen bonded to Y731 for the reactant and product, respectively; (B) direct-flipped-2 string, with no water hydrogen bonded to Y356 and two waters and one water hydrogen bonded to Y731 for the reactant and product, respectively; (C) mediated-flipped string, and (D) mediated-stacked string.

Author Manuscript Author Manuscript Author Manuscript Author Manuscript

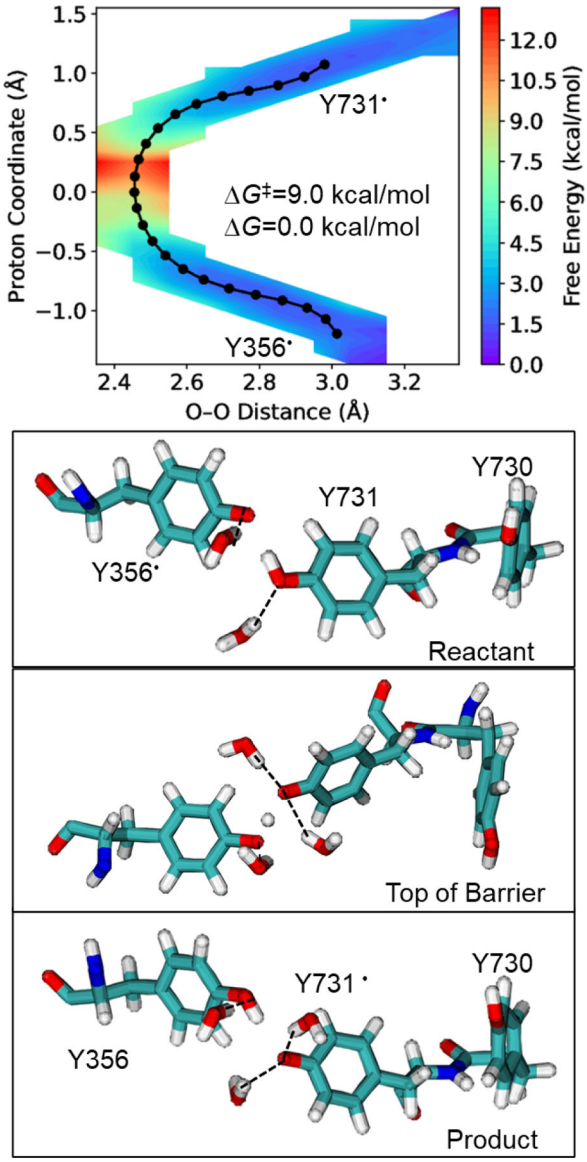

Figure 4.

Direct PCET mechanism for radical transfer from Y356 to Y731 in the flipped conformation. On the top is the two-dimensional free energy surface obtained from QM/MM free energy simulations, with the converged string shown in black. The proton coordinate is the difference between the Y731O−H and Y356O−H distances, where H is the transferring hydrogen. On the bottom are representative conformations for the reactant, top of the barrier, and product. Two water molecules hydrogen bond to the tyrosines in the reactant, and three water molecules hydrogen bond to the tyrosines at the top of the barrier and in the product. These interactions decrease the free energy barrier and reaction free energy. Hydrogen bonds are indicated by dashed lines.

Author Manuscript Author Manuscript Author Manuscript Author Manuscript

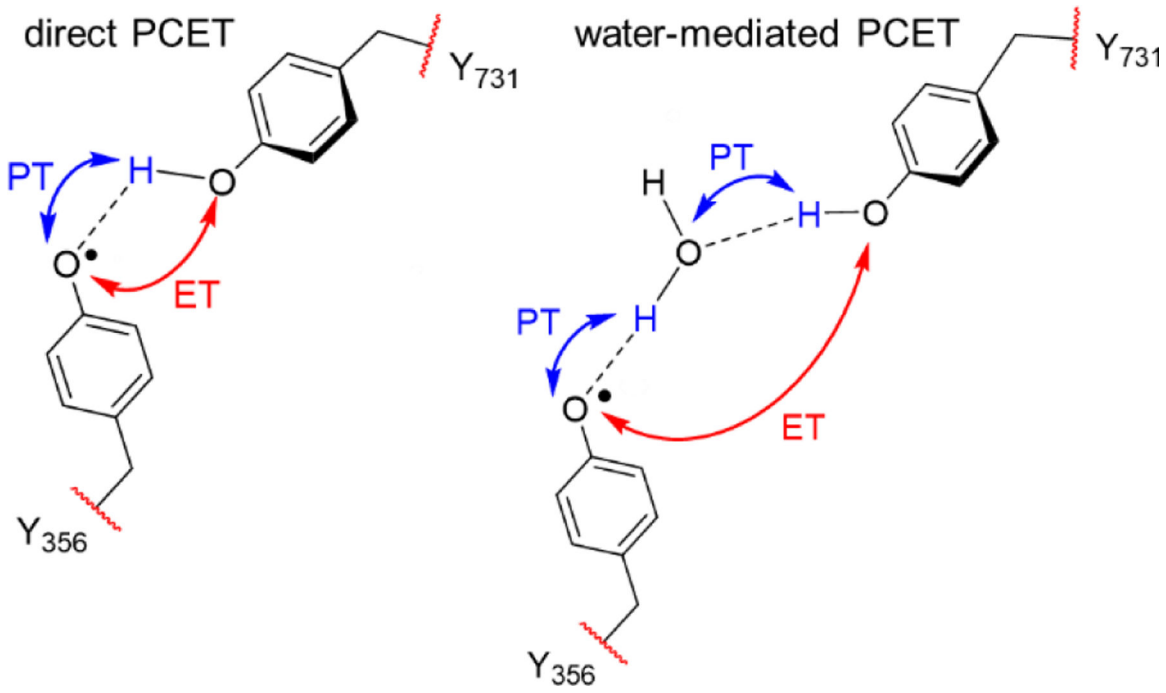

Scheme 1.

Schematic of Direct and Water-Mediated PCET Mechanisms between Y356 and Y731 in RNR without Depicting Protein and Solvent Environment.

Author Manuscript

Author Manuscript

Author Manuscript

Author Manuscript

Table 1.

Reaction Free Energies (ΔG) and Free Energy Barriers ($\Delta G^{\ddagger}$) for Radical Transfer from Y356 to Y731.

String	$\Delta G^{\ddagger}$ (kcal/mol)	ΔG (kcal/mol)
direct-flipped-1 [a]	9.0	0.0
direct-flipped-2 [a]	15.9	7.9
mediated-flipped [b]	26.9	17.3
mediated-stacked [b]	45.2	36.0

[a]Two independent strings were propagated for the direct PCET mechanism starting with different conformations of the surrounding water. The direct-flipped-1 string has one water hydrogen-bonded to Y356 throughout the entire reaction and one water hydrogen-bonded to Y731 in the reactant and two waters hydrogen-bonded to Y356 at the top of the barrier and product (Figure 3A). The direct-flipped-2 string has no water molecules hydrogen-bonded to Y356 throughout the entire reaction and two waters hydrogen-bonded to Y731 in the reactant and top of the barrier and one water hydrogen-bonded to Y731 in the product (Figure 3B). The strings simulating the direct PCET mechanism used three reaction coordinates (Figure S1).

[b]The strings simulating the water-mediated PCET mechanism used six reaction coordinates (Figure S1). Reactant and product conformations are shown in Figures 3C and 3D.

Author Manuscript

Author Manuscript

Author Manuscript

Author Manuscript

Table 2.

Comparison of Average Distances[a] and Number of Hydrogen Bonds between Water and Y356/Y731 for Strings Simulating Direct Radical Transfer from Y356 to Y731.

	Y356O–H (Å)	Y731O–H (Å)	O–O (Å)	# H-bonds Y356 [b]	# H-bonds Y731 [b]
direct-flipped-1					
Reactant	1.91	1.00	2.86	1	1
Top of barrier	1.17	1.30	2.46	1	2
Product	0.96	2.03	2.98	1	2
direct-flipped-2					
Reactant	1.91	0.97	2.86	0	2
Top of barrier	1.17	1.34	2.49	0	2
Product	0.97	1.97	2.92	0	1

[a]The distances between the transferring hydrogen and each of the tyrosine oxygens (denoted Y356O–H and Y731O–H) and between the oxygens of Y356 and Y731 (denoted O–O) were averaged over the final iteration for the images closest to the reactant, top of the barrier, and product for the two strings. The analogous distances are given for the two water-mediated mechanisms in Table S1.

[b]Number of hydrogen bonds between water and the specified tyrosine. Here a hydrogen bond is defined to have an O–O distance ≤ 3.0 Å and an O-H-O angle ≥ 135°.